Pulsars: A Key to Unlocking the Interstellar Medium

Laura M. Marschke

Faculty Sponsor: Shauna Sallmen, Department of Physics
Collaborator: Donald C. Backer, Department of Astronomy, UC-Berkeley

ABSTRACT

Located between the stars is a very low-density material consisting of gas and dust, called the interstellar medium (ISM). When new stars are born, they form from this material, and each time a star dies it enriches the ISM. This research studies the small-scale turbulent characteristics of the interstellar medium as the materials combine.

One way to determine characteristics of the ISM is to monitor signals from a pulsar. On average, pulse signals emitted by the pulsar are always the same; as they travel through the ISM they become slowed (dispersion delay) and scattered by the gas. The ISM affects the traveling signal and measuring the variations in these effects with time allows one to understand the properties of the intervening material. The pulse strength (flux), shape (scattering timescale) and arrival times tell us about the scintillation, scattering and electron-density properties of the ISM. We have studied the ISM using the Vela pulsar, located in the Vela Supernova Remnant. This paper presents observations of variations in the pulse strength, shape and arrival time at 327 MHz and 610 MHz. Our observations show a clear continuation of the decrease in intervening electron density seen by Hamilton *et al* (1985). This is interpreted as a wedge of plasma exiting the line of sight. An analysis of the small-scale flux and dispersion variations is also presented, and compared with various interstellar models.

INTRODUCTION

Despite seeming empty, the space between the stars in our Milky Way Galaxy is actually filled with a low-density gas called the interstellar medium (ISM). Stars form from this material and when they die they replenish it with elements heavier than the original hydrogen and helium. When stars explode (supernovae), the gas is disturbed and irregularities form. These new features are important in the formation process for the next generation of stars and thus, knowing more about the properties of the ISM allows for a better understanding of stellar and galactic evolution.

One way the properties of the ISM can be studied is by looking at radio waves produced by a pulsar. A pulsar is a neutron star that contains 1.4 solar masses packed into a sphere approximately 20 km in diameter, spinning rapidly (Lyne, 1998). Just as a lighthouse sweeps out a path of light as it rotates, a pulsar has a similar beam of radio emission. These beams are thought to be related to the strong magnetic field of the pulsar and are emitted from the poles. As the beams cross the line of sight a pulse is seen; on average these pulses have very stable shapes with predictable times of arrival. The pulses travel through, and are disturbed by, the interstellar medium between the pulsar and the earth. Since these objects are moving relative to each other, the pulse signal passes through different interstellar material at different times. Monitoring the changes in the pulsar signal allows us to investigate the properties of the ISM through which it has passed.

There are three measurements that must be made in order to measure these changes. The first is the dispersion delay. Radio waves interact with the electrons in the ISM causing the waves to travel slower. At lower frequencies waves travel slower and the pulses arrive later. By comparing the arrival times of the same pulse at two radio frequencies we can measure the electron-density of the ISM, which is called the dispersion measure (*DM*) given by the number of electrons along a particular line of sight:

$$DM \text{ (pc cm}^{-3}) = \int n_e dl.$$

By measuring the variations with time in the delay, we can measure the electron-density variations in the interstellar medium. The second measurement is interstellar scintillation. The variable-density ISM disrupts the phase of the pulsed radio signal. Constructive and destructive interference of the wave front results in an interference pattern through which the Earth moves. This is seen as a variation in time of the intensity (flux) of the signal. Lastly, there is interstellar scattering. This effect causes the shape of a pulse signal to broaden as it is scattered through the medium. The random density of ISM causes the signals to travel many different paths as they are refracted. When a signal takes a bent path it travels a longer distance to the telescope and thus the signal will arrive later. Averaging over all paths taken has the approximate effect of convolving the intrinsic pulse with an exponential decay of scattering time-scale τ. The value of τ depends on the radio frequency and the statistical properties of the medium through which the signal traveled. These three quantities (flux, τ and *DM*) vary with time and it is these variations that, when compared to models, allow for probing the properties of the interstellar medium.

Various models of the turbulent interstellar medium exist. Typically, the ISM variations are described by three-dimensional power laws of the form:

$$P(q) = C_n^2 q^{-\beta},$$

where q is $2\pi/l$ (l is the size scale) and where C_n^2 characterizes the strength of the scattering. The spectral index β determines the relationship between the amounts of turbulence on various spatial scales. These fluctuations introduce diffractive effects on small spatial scales, and refractive effects on large spatial scales. Both types of effects have been detected through pulsar observations. The Kolmogorov model, characterized by $\beta = 11/3$, is a power spectrum resulting from a cascading flow of wave energy from large to small scales. The energy is injected at an outer scale, and finally dissipates at an inner scale. This simplistic model explains some, but not all, interstellar effects of pulsars. A spectral index of $\beta \geq 4$ is required to explain some observations. A piece-wise power-law model, which increases in steepness ($\beta > 4$) at high frequencies can explain most observed effects (see Stinebring *et al* 2000 for a discussion and summary of these issues). However, uncertainty is introduced through assumptions about the location of the interstellar gas along the line of sight – a thin slab of material located at various distances will cause somewhat different effects, and a medium, which uniformly fills the line of sight, will be different again.

An example of this type of study involved the Crab pulsar. This pulsar is located in a supernova remnant and observations of extreme fluctuations in dispersion measure and τ have been interpreted in terms of plasma in the nebula. The supernova remnant behaves as a variable scattering screen unrelated to the general interstellar medium, which is more constant (Backer, 2000). A similar project also involved occasional observations taken at a much higher radio frequency and explains the Crab pulsar variations with ionized shells in the nebula (Lyne, 2001).

This research focuses on the Vela pulsar (PSR B0833-45) located within the Vela Supernova Remnant. The Vela supernova exploded about 11,000 years ago and is located approximately 815 light years away (Blair, 2006). The pulsar has a period of 89.3 ms. Since the Vela pulsar lies within the Vela supernova remnant; a single-component model of the ISM is unlikely to be completely successful. The supernova remnant fluctuations (unlikely to be identical to the fluctuations in the general ISM) will also contribute to the observed fluctuations. Recently, Zhou *et al* (2005) have compared a two-component model for interstellar scattering with the Stinebring *et al* (2000) results, obtaining a successful fit using $\beta = 4$.

From 1970 to 1984, P.A. Hamilton, P.J. Hall and M.E. Costa measured the *DM* of the Vela pulsar. They observed a dispersion measure decrease of 0.04 cm^{-3} pc yr^{-1} (Hamilton *et al*, 1985). This and other *DM* gradients have been attributed to wedges of plasma along the line of sight (Backer *et al*, 1993).

In the next section we present details of observations at 327 MHz and 610 MHz for the Vela Pulsar, as well as an outline of our data reduction techniques. We present our results for flux, τ and *DM* graphically, then analyze these results and relate to the properties of the ISM.

OBSERVATIONS AND DATA REDUCTION

Observations

The data used in this research were taken remotely from the 85-foot radio telescope in Green Bank, WV, using the Green Bank-Berkeley Pulsar Processor (GBPP) developed at the University of California at Berkeley. Data were gathered on a daily basis (with occasional interruptions) from mid-1995 through 2000; additional data were taken periodically in 2003 and 2004. This research focuses on data for the Vela Pulsar in the Vela Supernova Remnant, but other pulsar signals were recorded as well; these are often useful for calibration and comparison.

Two frequencies, ideal for studying the interstellar medium, were recorded: 327 and 610 MHz. Two to four scans at each frequency were collected daily. Each scan averaged many pulses together according to a timing model of the pulsar. The scans at 610 MHz were five minutes long and at 327 MHz they were 4.5 to 5 minutes. Both radio frequencies have data covering June 8, 1995 through August 28, 2000 (approximately daily) and October 30, 2003 through May 13, 2004 (occasionally). Figure 1 shows a typical scan at 610 MHz. There are 32 channels of frequency, which increase towards the top of the plot. Two polarizations are shown in the inner two panels. The far left and right sides show channel averages, allowing identification of interference. Each scan is displayed over one pulse period as labeled. Notice that the dispersion delay is apparent in each channel; the pulses arrive later at lower frequencies. The two lowermost panels are the averages over the channels, for each polarization, with the dispersion delay removed.

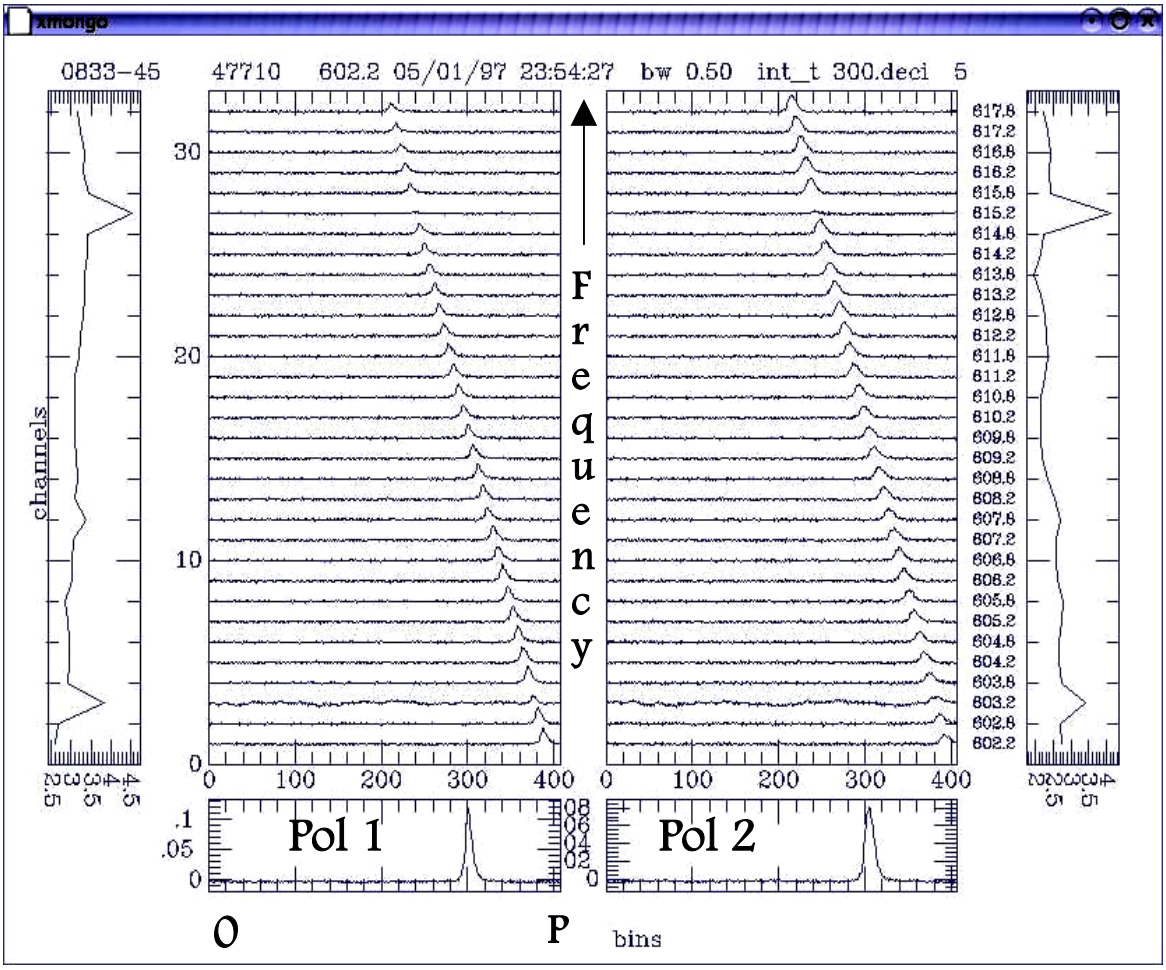

Figure 1. Typical scan at 610 MHz

Data Reduction

All observations were checked for interference or insufficient signal-to-noise ratios and such scans were eliminated. In addition, bad channels for each scan were noted and screened out. Anomalous data due to hardware and Y2K errors were also identified and dealt with. Once the data were reduced to a single pulse profile per scan, the flux, TOA and scattering time-scale were determined for each profile. A program called "scatfit" was used to read in a series of pulse profiles, fit a model to each pulse profile and output the parameters of the fit. The model consisted of a single Gaussian convolved with an exponential. The fit parameters were the area (related to pulsar flux), location (related to pulse TOA) of the Gaussian and the timescale of the exponential (corresponding to the scattering time-scale τ). Figure 2 shows the scan-by-scan flux and scattering time-scale versus date for the 327-MHz data and Figure 3 shows the same for the 610-MHz data. Both of these graphs show the span of data from

June 1995 to August 2000. Data from 2003 and 2004 have been excluded because of the large gap in time. Although there are multiple outliers, it is clear from the overall plots that these quantities are varying over the observed date range.

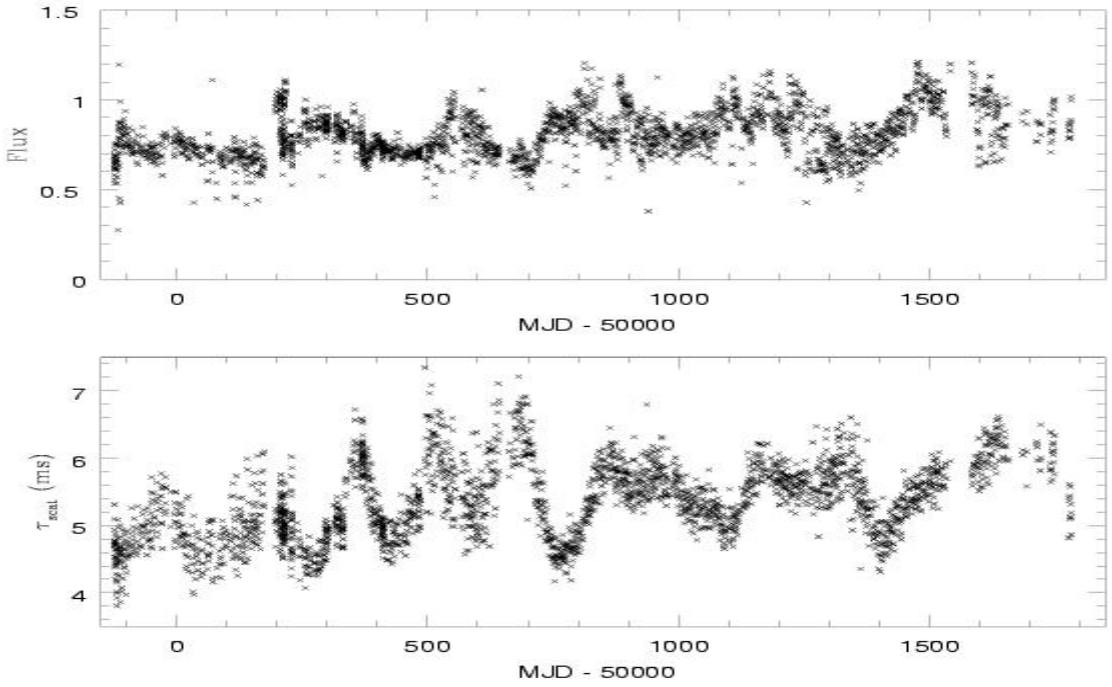

Figure 2. Flux and τ Versus Date (MJD) for 327 MHz

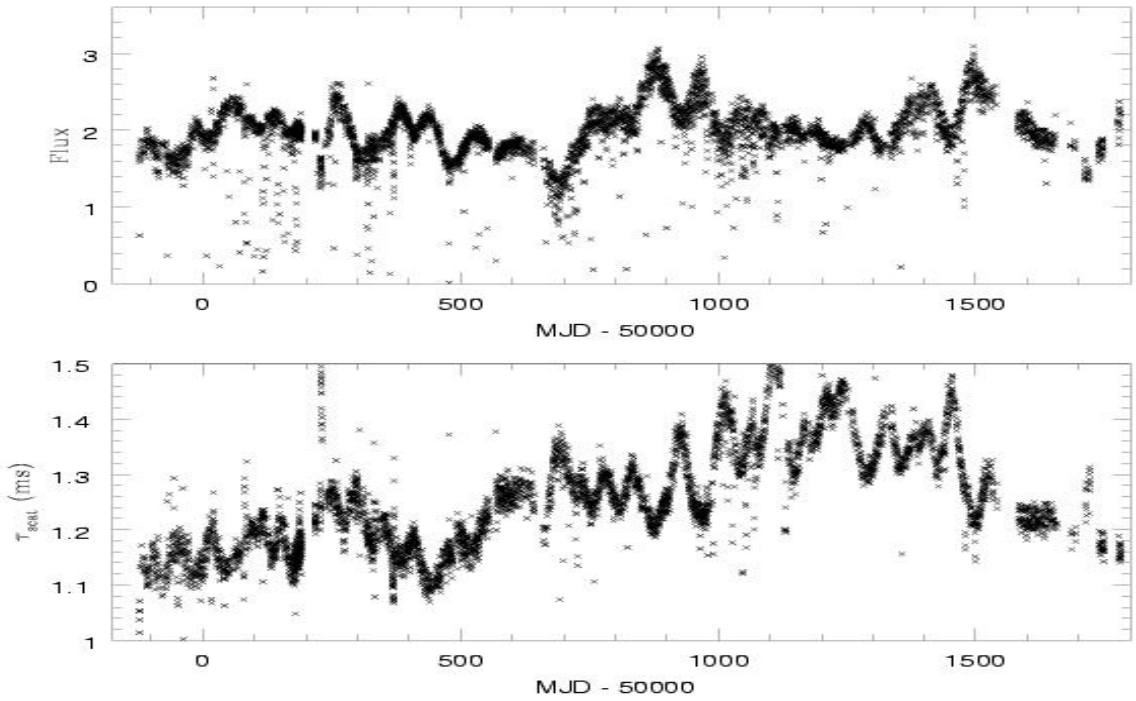

Figure 3. Flux and τ Versus Date (MJD) for 610 MHz

Accurate pulsar timing is required for dispersion measure determination. By comparing the TOAs from both frequencies, the *DM* may be calculated for each day. TOAs were compared to a timing model for this pulsar using the TEMPO[1] timing analysis software package. Due to glitches in October 1996 (MJD 50369) and September 1999 (MJD 51425) obtaining a successful timing model for the entire date range was time-consuming. The resulting timing residuals at the two radio frequencies (R_{610}, R_{327}), were used to calculate the dispersion measure:

$$DM = \frac{(R_{327} - R_{610})}{4150(\nu_1^{-2} - \nu_2^{-2})},$$

where ν_1 = 327 MHz and ν_2 = 610 MHz.

DATA ANALYSIS

Scattering Timescale

The average scattering timescale at each radio frequency was determined using the data shown in Figures 2 and 3. For the 327-MHz data, the mean scattering timescale τ_{327} was 5.3ms and the variance was 0.26. For the 610-MHz data, the mean scattering timescale τ_{610} was 1.26 ms and the variance was 0.009. In theory, the scattering timescales at the two frequencies should be related by $\tau(\nu_1) / \tau(\nu_2) = (\nu_1 / \nu_2)^{-\alpha}$, where $\alpha = 2\beta/(\beta - 2)$ (–4.4 for Kolmogorov spectrum). Our observations are significantly at variance with this prediction. Extrapolation of the measured τ_{327} to 610 MHz gives a predicted τ_{610} of only 0.4 ms, which should be just barely measurable. One possible explanation for the discrepancy is that our 610-MHz model profile did not include an intrinsic Gaussian component, so that τ_{610} is not measuring the actual interstellar component. Another explanation lies in the fact that interstellar scattering results in an exponential shape only for a thin-screen model of the ISM. It is possible that our approximation of this shape is too crude. Nonetheless, significant variations are seen in τ_{327}. Further analysis of this time-series will tell us about the refractive properties of the ISM.

Dispersion Measure

The top panel of Figure 4 shows the dispersion measure plotted versus date for June 1995 through September 1999. Although there are small-scale variations, overall a linear trend can be seen. Thus, a linear regression line was fit to the data with the equation:

$$DM(t) = A + B(t - t_0),$$

where t_0 corresponds to October 10, 1995 (MJD = 50000), A = 68.1881 ± 0.0004 cm^{-3} pc and B = – 0.0368 ± 0.0002 cm^{-3} pc yr^{-1}. Error bars are from the formal fit and do not include errors on *DM* or systematic errors.

This linear decrease was first noted by Hamilton *et al* (1985) and is believed to be a wedge of over-dense plasma leaving the line of sight (Backer & Wong 1999). In Figure 5, the green wedge represents an over-dense region of ISM. Due to motions of the pulsar and the sun, the line of sight changes with time. In 1970 the line of sight was in one direction and in 1999 a completely different direction. As shown, these two sightlines intersect different regions of the wedge where there are decreasing amounts of ISM, thus, a decrease in electron-density should be, and is, seen. In the bottom panel of Figure 4, the data points from Hamilton's observations have been plotted in conjunction with our results. Our linear regression line has been extrapolated backwards in time and when considering the error on Hamilton's measurements, it seems to be a reasonable continuation of their results. As mentioned, these features describe the large-scale variations in the ISM. Small-scale variations are due to smaller-scaled structures and turbulence.

The size of the interstellar region may be estimated by using the proper motion of the pulsar. From June 1995 to September 1999 (approximately 4.25 yrs) the transverse velocity is 62 ± 2 km s^{-1} (Dodson *et al*, 2003). This corresponds to a transverse length of about 3 x 10^{-4} pc or 60 AU. Then the dispersion measure decrease of about 0.16 cm^{-3} pc means the electron density surplus is about 600 cm^{-3}. If the region were smaller then the electron density would of course be greater.

[1] See http://pulsar.princeton.edu/tempo/ for a description of TEMPO.

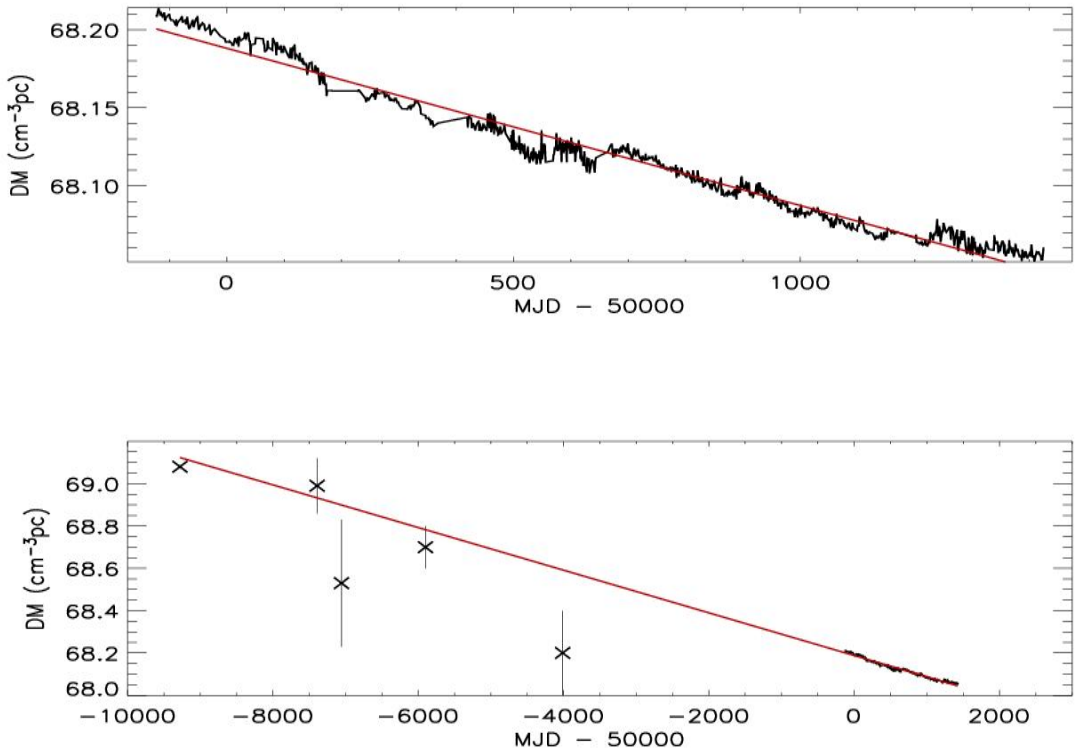

Figure 4. Dispersion Measure versus Date

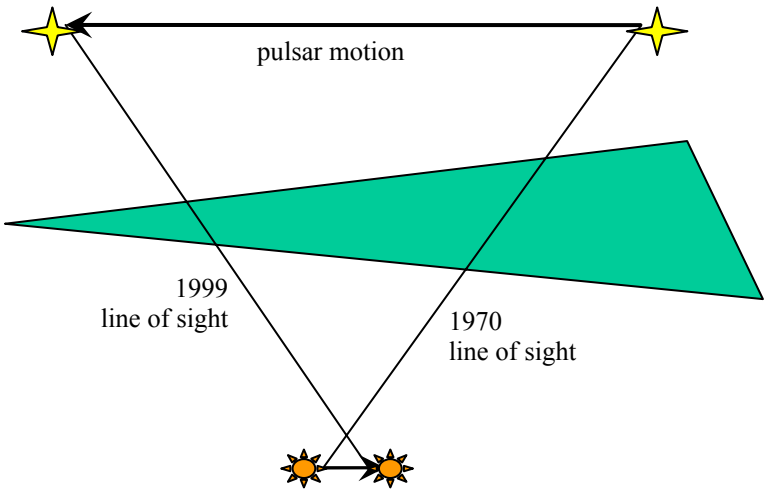

Figure 5. Plasma Wedge Diagram (not to scale)

Structure Functions

Small-scale variations are clearly seen in the flux, scattering-time scale and dispersion measure plots versus date. To further analyze observed variations in flux and *DM*, the structure functions were calculated; where structure functions quantify the variability in a data series. The value of the structure functions D on a time-scale t_0 for *DM* and flux (F) are as follows:

$$D_{DM}(t_0) = \langle [DM(t+t_0) - DM(t)]^2 \rangle / \langle DM(t) \rangle^2$$

$$D_F(t_0) = \langle [F(t+t_0) - F(t)]^2 \rangle / \langle F(t) \rangle^2,$$

where < > means an average over all data points separated by t_0. When calculated for all time-scales t_0, the structure function measures the typical variation of the data on each time-scale. Theoretically, we expect $D_{DM}(t_0) = k_1 t_0^{\beta-2}$ and $D_F(t_0) = k_1 t_0^{\gamma}$ where γ and β have theoretical values which depend on our model of turbulence in the ISM as well as the distribution of material along the line of sight.

In order to minimize scatter and to improve measurements of the structure functions for flux and τ, averaging over each day was done. The timing model obtained in order to determine the *DM* was used to create profiles averaged over one day. These allowed us to use scatfit to produce a single improved measurement of flux and scattering-time scale for each day. After this, obvious data outliers were removed using a median filter. The resulting day-averaged structure functions for the 327-MHz and 610-MHz flux are displayed in Figures 6 and 7. Note that in order to preserve clarity, we have plotted only selected lags.

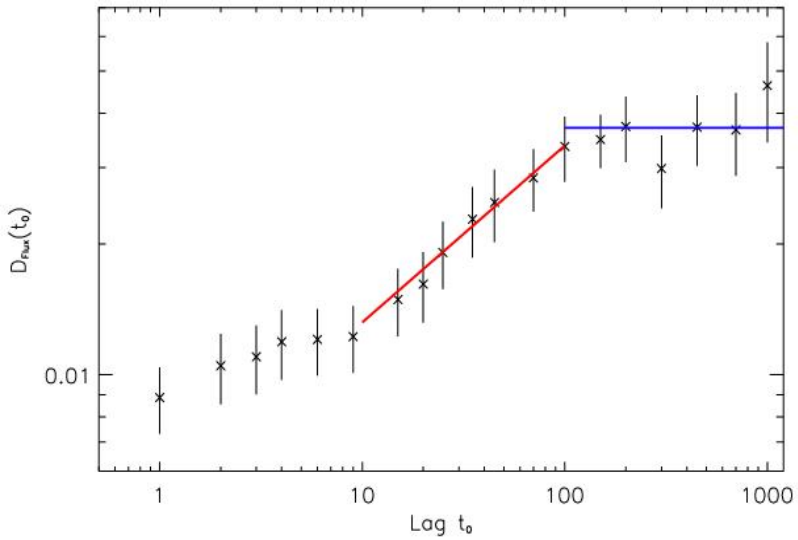

Figure 6. 327 MHz Flux Structure Function for PSR B0833-45

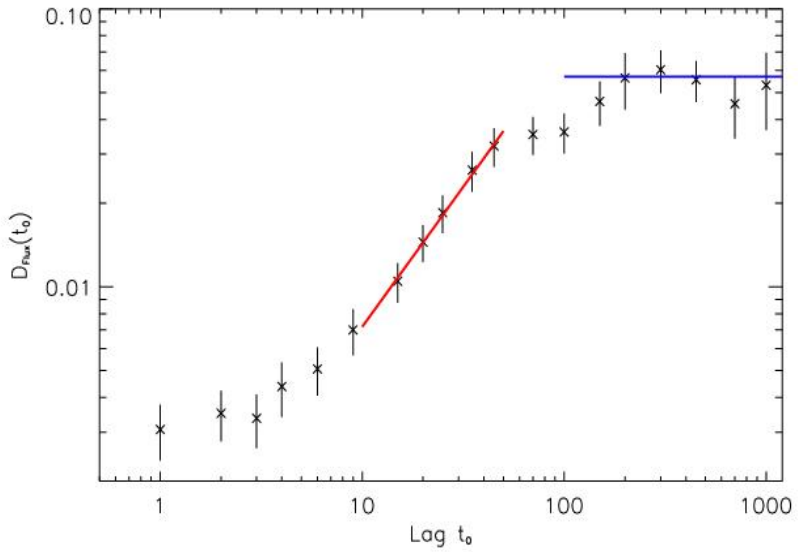

Figure 7. 610 MHz Flux Structure Function for PSR B0833-45

The relative transverse velocities of the Earth and the pulsar relate the time-scale of the observed fluctuations to the spatial scale of the ISM fluctuations. Therefore, large lags in the structure function plots correspond to large spatial scales. On a log-log plot, the shape of a structure function has three recognizable sections. The first is a "noise regime" on small scales, a linear structure regime on intermediate scales and saturation at the largest scales (see Stinebring and Condon, 1990 for a discussion). Because the interstellar turbulence has less power on small spatial scales, a "noise floor" is seen in the structure function for short timescales, when the fluctuations due to the ISM fall below other uncorrelated noise contributions. These include various sources of measurement error, as well as possible intrinsic variation in the flux of the pulsar (believed to be <5%; Stinebring *et al*, 2000). The noise floor lies at a value of twice the noise variance. Structure function saturation occurs on timescales significantly larger than the longest timescale in the interstellar process. This saturation value is equal to $2\sigma^2$ where σ^2 is the variance of the entire dataset (Stinebring *et al*, 2000).

The flux structure functions, displayed in Figures 6 and 7, clearly show these three regimes. The saturation level has been calculated and plotted as a blue line. The red line displays the results of a linear fit to the structure regime. An important parameter that may be determined from structure functions is the refractive timescale T_r, defined as the timescale at which the structure function takes on half the saturation value (see e.g. Kaspi and Stinebring, 1992).

The variances for the normalized flux time series are tabulated in Table 1, along with the associated saturation values and refractive timescales. The 610-MHz values are consistent with previous similar measurements by Stinebring *et al* (2000). As noted by these previous authors, the refractive timescale measured in this way is in contradiction both with theoretical predictions and the dominant timescale apparent in the top panel of Figure 3. Nonetheless, we confirm the result of these previous authors. This is the first measurement of these values at 327 MHz.

Table 1. Parameters Measured From Flux Observations

Observed Frequency	Variance of Normalized Flux	Saturation Value	Refractive Timescale	Slope (fit error)
327 MHz	0.0214	0.043	31 days	0.44 ± .03
610 MHz	0.0285	0.057	37 days	1.01 ± .03

The flux structure function is expected to take the form $D_F(t_0) \sim t_0^{\gamma}$, where $\gamma = 2$ for Kolmogorov turbulence within a thin screen, and $\gamma = \beta - 3$ for an even distribution along the line of sight. The 610-MHz slope is consistent with $\beta = 4$. There is a possible break in the structure function at a timescale of 9 days, corresponding to a length scale of 5×10^{12} cm. This is similar to the spatial scale for breaks as seen by Stinebring *et al* (2000) for other pulsars. However, we need to carefully remove the noise contribution in order to determine the significance of this feature.

It is somewhat surprising that the slope of the structure function at 327 MHz is so different from that at 610 MHz. We are currently investigating possible explanations. We intend to compare our new results to the two-component model of Zhou *et al* (2005). In the future, we will also compare the relationship between T_r at the two frequencies with theoretical predictions.

The *DM* structure function $D_{DM}(t_0)$, plotted in Figure 8, does not saturate. This indicates that the longest *DM* fluctuation timescale is much longer than the span of our data. This is reasonable, due to the long-term linear decrease discussed earlier. The slope of $D_{DM}(t_0)$ is expected to take the form $D_{DM}(t_0) \sim t_0^{\delta}$, where $\delta = 2$ for small timescales (corresponding to spatial scales less than the inner turbulence scale), 0 for spatial scales greater than the outer scale (not observed here), and $\beta - 2$ for scales in between. The observed structure function appears to have two different slopes, on different spatial scales. Between lags 20 and 100, the structure function has slope 0.95 ± 0.02, while for lags ≥ 150 the slope is 2.003 ± 0.006. This latter slope is consistent with $\beta = 4$, but the slope on the smaller scales is not. The smaller timescales correspond to spatial scales ≤ 5×10^{13} cm, or 3.5 AU. It is likely that small features in the supernova remnant are affecting the structure function on these scales.

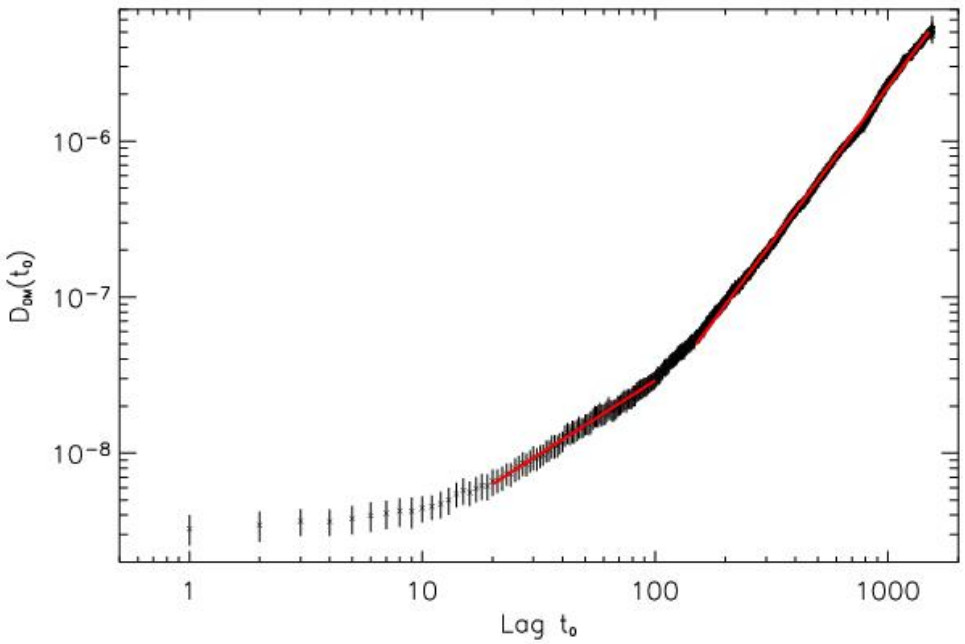

Figure 8. *DM* Structure Function for PSR B0833-45

CONCLUSION

Observing the flux, scattering time-scale and dispersion measure for the Vela pulsar from 1995 to 2000 has shown variations on large and small scales. The *DM* shows a continuation of the decrease seen by Hamilton *et al* (1985), due to an over-dense wedge of plasma exiting the sight line. The 610-MHz flux variations confirm previous work, but are in significant conflict with theoretical predictions. The first measurements of the 327-MHz flux structure function for this pulsar were presented. The dispersion measure structure function shows two slopes likely due to the Vela supernova remnant adding to the effects of the general interstellar medium.

ACKNOWLEDGEMENTS

Laura Marschke would like to thank the National Space Grant College and Fellowship Program as well as the Wisconsin Space Grant Consortium for their support and funding of this research. Dr. Shauna Sallmen would like to thank the University of Wisconsin – La Crosse for financial support through a faculty research grant. In addition, we would like to acknowledge Dr. Donald C. Backer from the University of California at Berkeley as a collaborator on this project.

REFERENCES

Backer, D.C., Hama, S., Van Hook, S. & Foster, R.S. 1993. *Temporal Variations of Pulsar Dispersion Measures*. The Astrophysical Journal, **404**, 636

Backer, D.C., Wong, T. 1999. *Interstellar Weather – Radio Wave Propagation Through the Turbulent Ionized Interstellar Medium* in *Pulsar Timing, General Relativity and the Internal Structure of Neutron Stars,* p39. Ed. Z. Arzoumanian, F. Van der Hooft, and E.P.J. van den Heuvel (Amsterdam: KNAW)

Backer, D.C., Wong, T. & Valanju, J. 2000. *A Plasma Prism Model for an Anomalous Dispersion Event in the Crab Pulsar*. The Astrophysical Journal, **543**, 740

Blair, Bill. *Bill Blair's Vela Supernova Remnant File*. Johns Hopkins University. http://fuse.pha.jhu.edu/~wpb/hstvela/hstvela.html. 11 May 2006.

Dodson, R., Legge, D., Reynolds, J.E. & McCulloch, P.M. 2003. *The Vela Pulsar's Proper Motion and Parallax Derived From VLBI Observations*. The Astrophysical Journal, **596**, 1137

Hamilton, P.A., Hall, P.J. & Costa, M.E. 1985. *Changing Parameters Along the Path to the Vela Pulsar*. Monthly Notices of the Royal Astronomical Society, **214**, 5

Kaspi, V.M., Stinebring, D.R. 1992. *Long-Term Pulsar Flux Monitoring and Refractive Interstellar Scintillation*. The Astrophysical Journal, **329**, 530

Lyne, A.G., Graham-Smith, F. *Pulsar Astronomy*. Eds. A. King, D. Lin, S. Maran, J. Pringle, and M. Ward. Cambridge University Press. Cambridge, United Kingdom. 1998.

Lyne, A.G., R. S. Pritchard, F. Graham-Smith. 2001. *Pulsar Reflections Within the Crab Nebula*. Monthly Notices of the Royal Astronomical Society, **321**, 67

Stinebring, D.R., Condon, J.J. 1990. *Pulsar Flux Stability and Refractive Interstellar Scintillation*. The Astrophysical Journal, **352**, 207

Stinebring, D.R., Smirnova, T.V., Hankins, T.H., Hovis, J.S., Kaspi, V.M., Kempner, J.C., Myers, E. & Nice, D.J. 2000. *Five Years of Pulsar Flux Density Monitoring: Refractive Scintillation and the Interstellar Medium*. The Astrophysical Journal, **539**, 600

Zhou, A.Z., Esamdin, A. & Wu, X.J. 2005. *Two-Component Model for the Interstellar Scattering in Direction to the Vela Pulsar*. Astronomy & Astrophysics, **438**, 909